A R C H I V E S O F M E T A L L U R G Y A N D M A T E R I A L S
Volume 58 2013 Issue 2
DOI: 10.2478/amm-2013-0018

A. DUSZOVÁ*, J. MORGIEL**, Z. BASTL***, J. MIHÁLY****, J. DUSZA*****

CHARACTERIZATION OF CARBON NANOFIBERS/ ZrO_2 CERAMIC MATRIX COMPOSITE

CHARAKTERYSTYKA KOMPOZYTU O OSNOWIE CERAMICZNEJ MODYFIKOWANEJ WŁÓKNAMI WĘGLOWYMI

Carbon micro/nanofibers prepared by catalytic chemical vapor deposition have been characterized in the form of powders and in the form of filaments, intercorporated in the matrix of ZrO_2. Scanning electron microscopy, transmission electron microscopy, high resolution electron microscopy, electron spectroscopy for chemical analysis and Raman spectroscopy have been used. The outer diameter of the fibers varied from 50 nm to 600 nm with an average diameter of 120 nm, length from several micrometers to several tens of micrometers and inner diameters from 20 nm to 230 nm. Two types of fibers have been identified; cylindrical which consists of a distinct graphite layers parallel to the fiber axes and bamboo – shaped fibers with walls which are built from domains with different orientations of graphite layers. The fibers contain 99.05 at.% carbon and 0.95 at.% oxygen with a binding energy of O (1s) electrons of 532.7 eV which corresponds to carbon in C-O bonds. In the first-order Raman spectra, the position of the band G was found at 1600 cm^{-1} and D at 1282 cm^{-1}. The CNFs in ZrO_2 + CNFs composite have been relatively well dispersed, however clusters of CNFs together with porosity are present as a result of the difficulty of dispersing, too. TEM and HREM revealed that the CNFs are usually located at the grain boundaries of ZrO_2 in the form of undamaged nanofibers or disordered graphite.

Keywords: Carbon nanofibers, Nanocomposites, Transmission electron microscopy, High resolution transmission electron microscopy, Raman spectroscopy

Włókna węglowe przygotowane metodą osadzania z par (tzw. Chemical Vapour Deposition), były badane bezpośrednio po wytworzeniu oraz po wprowadzeniu do osnowy ceramicznej metodami elektronowej mikroskopii skaningowej, transmisyjnej oraz spektroskopii ramanowskiej. Średnica włókien wahała się pomiędzy 50 nm, a 600 nm przy średniej wartości ~120 nm, podczas gdy ich długość wynosiła od kilku do kilkudziesieciu mikrometrów. Identyfikowano dwa rodzaje budowy włókien, tj. cylindryczne oraz z wewnętrznymi przekładkami typu „łodygi bambusa". Włókna węglowe zawierały do 0.95 at. % tlenu o energi wiązania O (1s) ~532.7 eV, co odpowiada wiązaniu C-O. Na pierwszym widmie Ramana pasmo G identyfikowano dla 1600 cm^{-1}, a pasmo D dla 1282 cm^{-1}. Badania kompozytu wykazałay równomierny rozkład włókien w ceramicznej osnowie. W sąsiedztwie większych aglomeratów stwierdzono tendencje do występowania pustek. W czasie spiekania przeważająca część włókien zachowała swoją rurkową strukturę, natomiast pozostały materiał węglowy uległ przemianie do słabo uprządkowanych struktur grafitu lub nawet uległ amorfizacji.

1. Introduction

During the last years extensive research has been performed in the field of synthesis and characterization of filamentous carbons over the world prepared using different processing route [1,2]. Beside the most investigated carbon nanotubes (CNTs), other filamentous carbons have also been developed as well, e.g. nanofibers [3-5]. Carbon nanofibers (CNFs) are cylindrical or conical structures that have diameters varying from a few to hundreds of nanometers and lengths ranging from less than a micron to millimeters. The internal structure of carbon nanofibers varies and is comprised of different arrangements of modified graphene sheets. The main distinguishing characteristic of nanofibers from nanotubes is the stacking of graphene sheets of varying shapes [6].

During the last few years there is a growing interest in using carbon nano-filaments in the form of CNTs and CNFs with the aim to improve the mechanical and functional properties of ceramic/CNTs of ceramic/CNFs composites compared to the monolithic material [7-9].

Different techniques/methods have been used for the characterization of CNTs and CNFs during the last decade, included scanning electron microscopy (SEM), transmission electron microscopy (TEM), high resolution transmission electron microscopy (HRTEM), electron spectroscopy for chemical analysis (ESCA), Raman Spectroscopy, X-ray photoelectron spec-

* INSTITUTE OF MATERIALS RESEARCH, SLOVAK ACADEMY OF SCIENCES, WATSONOVA 47, 040 01 KOSICE, SLOVAKIA
** INSTITUTE OF METALLURGY AND MATERIALS SCIENCE OF POLISH ACADEMY OF SCIENCES, REYMONTA 25, 30 059 KRAKOW, POLAND
*** J. HEYROVSKÝ INSTITUTE OF PHYSICAL CHEMISTRY, ACADEMY OF SCIENCES OF THE CZECH REPUBLIC, DOLEJŠKOVA 3, 182 23 PRAGUE 8, CZECH REPUBLIC
**** CHEMICAL RESEARCH CENTER, HUNGARIAN ACADEMY OF SCIENCES, H-1025 PUSZTASZERI ÚT 59-67, BUDAPEST, HUNGARY
***** ÓBUDA UNIVERSITY, DONÁT BÁNKI FACULTY OF MECHANICAL AND SAFETY ENGINEERING, NÉPSZÍNHÁZ STREET 8, 1428 BUDAPEST, HUNGARY

troscopy, etc [10]. SEM is commonly used for the characterization of the morphology of the CNTs and CNFs in the form of powders but in the form as structural element in bulk material, too [11]. Determination of the structures of CNTs within the bundles, for example the helicity, can be obtained using TEM coupled with electron diffraction [12]. X-ray photoelectron spectroscopy (XPS) can be used to get information on the chemical structure of CNTs, for example to study the incorporation of nitrogen into carbon nanotubes [13], sidewall functionalization of SWNTs by fluorination [14]. Infrared spectroscopy is often used to determine impurities remaining from synthesis or molecules capped on the CNTs surface. The allotropic forms of carbon such as fullerenes, carbon nanotubes, amorphous carbon, polycrystalline carbon, etc, are active in Raman spectroscopy. For that reason this method is one of the most powerful tools for characterization of CNTs which doesn't need special sample preparation, being in such a way a fast and nondestructive analysis [15].

The aim of the present contribution is to characterize a new ceramic matrix functional composite of ZrO_2+ CNFs, using different characterization techniques and methods.

2. Experimental material and methods

The experimental material was prepared by catalytic chemical vapor deposition (CCVD), which is equivalent to catalytic deposition from the gaseous phase (ElectrovacAG) supplied for the analysis by EMPA, Switzerland. The bulk ZrO_2+ 2 vol% CNFs composite has been prepared by hot pressing at EMPA, Switzerland [16].

Field emission SEM (JEOL 7000F) was used for examination of the length, diameter and morphology of the carbon nanofibers in the form of powders and for the distribution of CNFs in the matrix of bulk material. Specimens for microstructure examination of bulk material were prepared by diamond cutting, grinding, polishing and thermal etching at a temperature of 1250°C in air and coated by carbon before the examination.

TEM and HRTEM were employed to observe the crystal structure and graphite layer arrangement. The TEM specimens of the CNFs powder have been prepared by dispersing the CNF in acetone ultrasonic bath and dropping a suspension onto a carbon lace Cu grid. In the case of hulk specimens thin foils were used, prepared using focused ion beam (FIB) Quanta 3D system equipped with Omniprobe lift-out system. TECNAI G^2 FEG SuperTWINN (200kV) transmission-scanning electron microscope equipped with both side-entry wide angle SIS and on-axis bottom mounted Gatan 2K CCD cameras was used for the examination of both types of specimens.

In order to provide information on chemical composition and carbon bonding the CNFs powder was examined by XPS and XAES methods using a VG ESCA3 MkII electron spectrometer. The spectra were recorded with Al Kα radiation and an electrostatic hemispherical analyzer operated in the fixed analyzer transmission mode.

Raman measurements were performed by a BioRad (Digilab) FT-Raman spectrometer using an excitation with 1064 nm radiation from a Nd:YAG laser at 200 mW. To reduce thermal emission during spectra acquisition and to gain acceptable quality Raman spectra, the samples were mixed and ground with spectroscopic grade potassium bromide (KBr). Spectra were recorded at 4 cm^{-1} resolution with white light correction by co-addition of 2048 individual spectra. The investigated sample area is approx. 2 mm, the estimated penetration depth for carbon materials (optically opaque) is around few tens nm [17]. For data manipulation Grams/32 (Galactic Industries Corporation) software package was used, band positions were analyzed using a mixed Gaussian-Lorentzian curve-fitting procedure.

3. Results and discussion

3.1. Characterization of CNF powders

The morphology of the carbon nanofibers is illustrated in Fig. 1 a,b. Two basic types of nanofibers have been identified by SEM observation; cylindrical hollow rope – type tubes, usually with free ends and smooth surface and bamboo shaped nanofibers with a waved surface The cylindrical, rope – like shaped fibers exhibits tubular structure with an outer diameter of 50 – 250 nm and inner diameter from 20 nm to 230 nm [18]. The study of the surface morphology of the fibers revealed that the fibers with smaller diameters are smoother compared to the fibers with larger diameters. Lee *et al.* [19] investigated the surface morphology of hollow and solid as received, heat – treated and CVD surface treated fibers and found that the solid fibers exhibited a rougher surface compared to the hollow fibers in all form. Measurement and statistical evaluation of the distribution of the diameters of nanofibers show their diameter changing from 50 to 600 nm with the average diameter equal to 120 nm.

Results of TEM, Fig. 1b, are in a good agreement with the results of SEM and it can be seen that in the case of straight pipe-shaped fibers the wall is smooth and uniform and consists of a distinct sandwich of graphite layers. In this case the graphite layers are parallel to the axes of the fibers and forming usually defect-free material. The bamboo – shaped fibers are composed of multi – walled graphite structure and the bamboo sections have a size parallel with the axes of the fibers 2-3 times larger compared to the outer diameter of the fibers. It seems that the carbon diffusion was not continuous with all fibers during their growth, leading to a pulsed growth which translated into a periodic variation of the fiber diameter. Such bamboo – shaped fibers are composed of hollow segments of a size approximately 100 nm deliminated by curved stacking of carbon sheets. Bamboo-shaped carbon-nitrogen nanotubes have been prepared by Lee [20] using pyrolysis of iron pentacarbonyl and acetylene mixture with ammonia, and by pyrolisis of melamine with NaN_3-Fe-Ni and Ni catalyst, respectively. According to the results of Lee *et al.* [20], the nitrogen doping leads to the origin of the bamboo-like structure and results in the degraded crystallinity of graphite sheets. By TEM they found that in the bamboo-like CN nanotubes the wall thickness increases due to the generation of compartment layers, but the outer diameter remains constant. This is different compared to the bamboo-like carbon nanotubes characterized in the present investigation, when the outer diameter of

the nanofibers increase during the generation of compartment layers due to the changed orientation of the graphite sheets.

Result of Raman scattering in the 1800-1000 cm^{-1} wavenumber region is presented in Fig. 1c. The spectra is dominated by the two characteristic first-order Raman bands of carbonaceous materials: the so called *G-band* at 1600 cm^{-1} (E_{2g} mode of graphitic layers, produced from the high degree of carbon materials and generally used to identify well-ordered CNTs) and the *D-band* at 1282 cm^{-1} (disorder-induced phonon mode, related to disordered structures in carbon materials) [21]. The additional two weak noisy bands observed at around 1150 and 1370 cm^{-1} can be assigned to the mixed bonds between sp2- and sp3-carbon [22] and to semi-circle breathing mode of smaller aromatic ring systems [23], both typical for amorphous carbon structures.

Zang *et al*. [24] recently studied the characteristics of as-received and graphitized vapor – grown carbon nanofibers with the outer diameter similar as in the present study by Raman spectroscopy at excitation wavelength of 632.8 nm. They found that the first order Raman spectrum composed of two main peaks, around 1340 cm^{-1} and 1590 cm^{-1} for the non-graphitized and 1340 cm^{-1} and 1582 cm^{-1} for graphitized nanofibers, respectively. The ratio of the intensity of D-band to G-band was 0.8 for non-graphitized and 0.37 for graphitized carbon nanofibers. The results of the ESCA analysis are illustrated in Fig. 1d. Survey spectra revealed the presence of carbon and a small amount of oxygen. The O/C atomic concentration ratio calculated from integrated intensities of O (1s) and C (1s) photoemission lines was equal to 0.01. According to the results, the analyzed carbon nanotubes consist of 99.05 at.% carbon and 0.05 at.% oxygen. The binding energy of O (1s) electrons, 532.7 eV corresponded to carbon in C – O bonds.

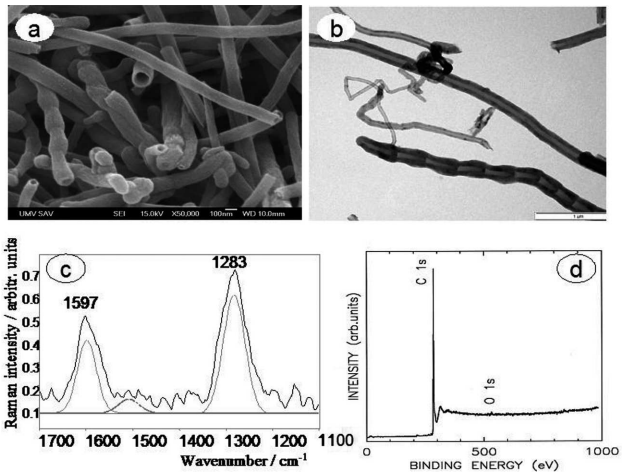

Fig. 1. Results of the characterization of CNF powders. (a) SEM image of CNFs; (b) TEM micrograph of the CNFs; (c) Raman spectra of CNFs at 1064 nm excitation wavelength; (d) Survey ESCA spectra measured in the interval of 0 – 1000 eV

3.2. Characterization of CNFs in ZrO_2-CNFs composite

According to the results of microstructure examination the hot pressed monolithic zirconia was fully dense but the ZrO_2- 2.0 vol% CNF composite contained porosity, which was associated with clustering of the carbon nanofibers. The CNF clusters observed on the polished and fracture surfaces of the composite samples are probably the result of the difficulties at the mixing of the powders similarly as in the case of ceramic – CNTs composites, (Fig. 2). The size of the clusters varied from a few microns up to approximately 40 μm, and porosity was always connected with these clusters. The presence of such clusters and the associated porosity is the main reason of the lower density of the composite compared to its theoretical density. The observation of the starting CNFs revealed relatively large hard agglomerates, which were not removed before the mixing and remained in the microstructure in the form of clusters.

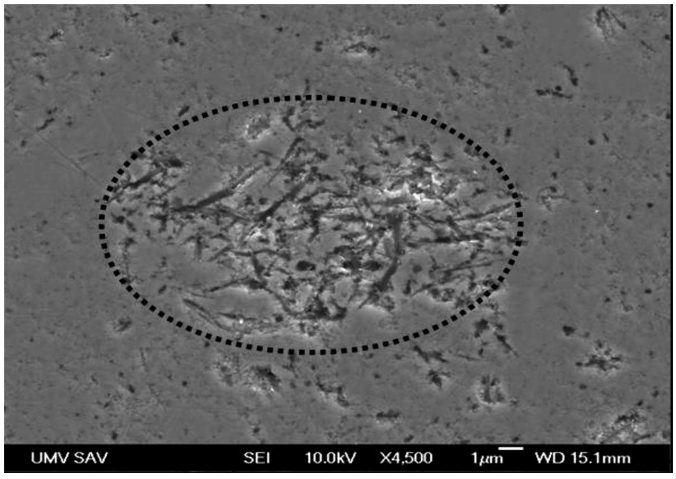

Fig. 2. Cluster of CNFs in the ZrO_2- 2.0 vol% CNFs composite

Taking to the consideration the differences in shape and dimension/aspect ratio between the CNTs and CNFs, the preparation of cluster free composites (in the case of powders without hard agglomerates) seems to be easier with CNFs.

The microstructure of the composite consists of a similar or an even smaller grained matrix with relatively well dispersed CNFs (pores with shape/orientation indicating the locations of the burned out CNFs during the thermal etching) in the matrix (Fig 3a). This is an indication that the CNFs hinders the matrix grain growth in similar way as the CNTs, which can results in improved mechanical properties.

Characteristic grain boundary in the zirconia/CNF composite is illustrated in Fig. 3b.

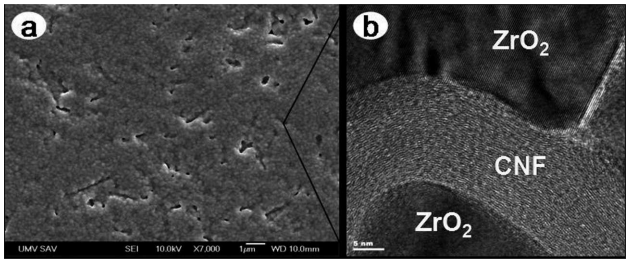

Fig. 3. (a) Microstructure of the ZrO_2- 2.0 vol% CNFs composite and (b) HRTEM image of the characteristic CNF at the ZrO_2/ZrO_2 boundary

From this is evident that the microstructure of ceramic – CNF composites is basically different comparing to ceramic – CNT composites due to the ratio of the average ceramic grain diameter and the average diameter of CNTs or CNFs. In the

case of CNTs it is approximately 20 (considering a grain size of 500 nm and CNT diameter of 25 nm), while for CNFs it is approximately 5 (considering a grain size of 500 nm and CNF diameter of 100 nm). In the present investigation it is even lower, approximately one, because of the very small grain size of the zirconia matrix. This means that the matrix grains are located around the CNFs, and not the CNFs are located around or inside the zirconia grains. According to detailed HREM study in the composite beside the CNFs there exists a second graphite based intergranular phase in the form of disordered graphite, resulting probably from the degradation of CNTs during the powder preparation and the sintering routes. This is in full agreement with Vasiliev *et al.* [25] who during the study of Al_2O_3/10 vol.% SWCNTs system found at the alumina boundaries disordered graphite which, according to them, formed during the SPS process.

It seems that the shape, size and surface characteristics of the carbon based nano-fillers (CNTs, CNFs, graphene platelets) will significantly influence the mechanical (strength, fracture toughness, etc.) and functional (electrical conductivity, etc.) properties of ceramic –carbon filler composites and to understand this influence further investigation is required.

4. Conclusions

The main results can be concluded as follow:

- Two types of fibers have been identified; cylindrical which consists of a distinct graphite layers parallel to the fiber axes and bamboo – shaped fibers with walls which are built from domains with different orientations of graphite layers.
- The fibers contain 99.05 at.% carbon and 0.95 at.% oxygen with a binding energy of O (1s) electrons of 532.7 eV which corresponds to carbon in C-O bonds. In the first-order Raman spectra, the position of the band G was found at 1600 cm^{-1} and D at 1282 cm^{-1}
- During the preparation of ZrO_2-CNFs composite the CNFs have been relatively well dispersed in the matrix, however clusters of CNFs together with porosity are present in the composite, too.
- TEM and HRTEM revealed that the CNFs in the composite are located at the grain boundaries of ZrO_2 in the form of undamaged nanofibers or disordered graphite.

Acknowledgements

The work was supported by projects Slovak Grant Agency for Science, grant No. 2/7914/27 and 2/0122/12, by the Integrisk EU 6FP, NanoCEXmat I. ITMS no:262200120019, NanoCEXmat II., ITMS no: 26220120035, CeKSiM, ITMS no:26220120056 and project COST MP 0902.
A.D. thanks the support of KMM-MIN.

REFERENCES

[1] S. Iijima, Helical microtubles of graphitic carbon, Nature **354**, 56-58 (1991).
[2] T.W. Ebbesen, P.M. Ajayan, Large scale synthesis of carbon nanotubes, Nature **358**, 220-222 (1992).
[3] J.H. Hafner, C.L. Cheung, C.M. Lieber, Direct Growth of Single-Walled Carbon Nanotube, Scanning Probe Microscopy Tips, J. Am. Chem. Soc. **121**, 9750-9751 (1999).
[4] S. Takenaka, S. Kobayashi, H. Ogihara, K. Otsuka, Ni/SiO_2 catalyst effective for methane decomposition into hydrogen and carbon nanofiber, J. Catal. **217**, 79-87 (2003).
[5] G. Zou, D. Zhang, Ch. Dong, H. Li, K. Xiong, L. Fei, et al., Carbon nanofibers: Synthesis, characterization and electrochemical properties, Carbon **44**, 828-832 (2006).
[6] A.V. Melechko, V.I. Merkulov, T.E. McKnight, M.A. Guillorn, K.L. Klein, D.H. Lowndes, et al., Vertically aligned carbon nanofibers and related structures: Controlled synthesis and directed assembly, J. Appl. Phys. **97**, 041301 (2005).
[7] J.W. An, D.H. You, D.S. Lim, Tribological properties of hot-pressed alumina – CNT composites, Wear **255**, 677-681 (2003).
[8] Cs. Balazsi, Z. Kónya, F. Wéber, L.P. Biró, P. Arató, Preparation and Characterization of Carbon Nanotube Reinforced Silicon Nitride Composites, Mat. Sci. Eng. C **23**, 1133-1137 (2003).
[9] A.K. Kothari, K. Jian, J. Rankin, B.W. Sheldon, Comparison Between Carbon Nanotube and Carbon Nanofiber Reinforcements in Amorphous Silicon Nitride Coatings, J. Am. Ceram. Soc. **1-4**, (2008).
[10] A. Merkoci, Carbon nanotubes in analytical sciences, Microchim Acta **152**, 157-74 (2006).
[11] N. Yao, Z.L. Wang, Microscopy for nanotechnology, Kluwer academic publishers, USA, (2005).
[12] J. Cowley, F. Sundell, Nanodiffraction and dark-field STEM characterization of single walled carbon nanotube ropes, Ultramicroscopy **68**, 1-12 (1997).
[13] R. Droppa, P. Hammer, A.C.M. Carvalho, M. Dos Santos, F. Alvarez, Incorporation of nitrogen in carbon nanotubes. Non-Cryst Solids **299-302**, 874-879 (2002).
[14] Y.S. Lee, T.H. Cho, B.K. Lee, J.S. Rho, K.H. An, Y.H. Lee, Surface properties of fluorinated single-walled carbon nanotubes, J. Fluorine Chem. **120**, 99-104 (2003).
[15] E.F. Antunes, A.O. Lobo, E.J. Corat, V.J. Trava-Airoldi, A.A. Martin, C. Veríssimo, Comparative study of first – and second – order Raman spectra of MWCNT at visible and infrared laser excitation, Carbon **44**, 2202-2211 (2006).
[16] J. Dusza, G. Blugan, J. Morgiel, J. Kuebler, F. Inam, T. Peijs, M.J. Reece, V. Puchý, Hot pressed and spark plasma sintered zirconia/carbon nanofiber composites, In Journal of the European Ceramic Society **29**, 3177-3184 (2009).
[17] R. Longtin, L.P. Carignan, C. Fauteux, P. Therriault, J. Pegna, Selective area synthesis of aligned carbon nanofibers by laser assisted catalytic chemical vapor deposition, Diamond Relat. Mater. **16**, 1541-1549 (2007).
[18] V. Puchý, P. Tatarko, J. Dusza, J. Morgiel, Z. Bastl, J. Mihály, Characterization of carbon nanofibers by SEM, TEM, ESCA and Raman spectroscopy, In Kovové materiály **48**, 379-385 (2010).
[19] S. Lee, T.R. Kim, A.A. Ogale, M.S. Kim, Surface and structure modification of carbon Nanofibers, Synth. Met. **157**, 644-650 (2007).
[20] C.J. Lee, S.C. Lyu, H.W. Kim, J.H. Lee, K.I. Cho, Synthesis of bamboo shapedcarbon nitrogen nanotubes using C_2H_2-NH_3-$Fe(CO)_5$ system, Chem. Phys. Letters **359**, 115-120 (2002).

[21] M.S. Dresselhaus, G. Dresselhaus, R. Saito, A. Jorio, Raman spectroscopy of carbon nanotubes. Physics Reports **409**, 47-99 (2005).

[22] A.C. Ferrari, J. Robertson, Resonant Raman spectroscopy of disordered, amorphous, and diamond-like carbon, Phys. Rev. B **64**, 075414-1-075414-13 (2001).

[23] X. Li, J.I. Hayashi, C.Z. Li, FT-Raman spectroscopic study of the evolution of char structure during the pyrolysis of a Victorian brown coal, Fuel **85**, 1700-1707 (2006).

[24] Y. Zang, Y.H. Tang, L.W. Lin, E.L. Zhang, Microstructure transformation of Carbon Nanofibers during graphitization, Trans. Nonferrous Met. Soc. **18**, 1094-1099 (2008).

[25] L.A. Vasiliev, R. Poyato, P.N. Padture, Single-wall carbon nanotubes at ceramic grain boundaries, Scr. Mater. **56**, 461 (2007).

Received: 20 January 2013.